



RESEARCH ARTICLE

Sensitivity of WRF Cloud Microphysics to Simulations of a Convective Storm Over the Nepal Himalayas

Rudra K. Shrestha^{1,*}, Paul J. Connolly² and Martin W. Gallagher²

¹*Canadian Center for Climate Modelling and Analysis (CCCma), Environment and Climate Change Canada (ECCC), Victoria, British Columbia, Canada*

²*Center for Atmospheric Science, School of Earth, Atmospheric and Environmental Sciences, The University of Manchester, Manchester, UK*

Received: December 13, 2016

Revised: February 16, 2017

Accepted: March 10, 2017

Abstract:

Background:

This paper investigates sensitivity of bulk microphysical parameterization (BMP) schemes within the Weather Research and Forecasting (WRF) model to simulate a convective storm that generally evolves during pre-monsoon season (March – May) across the foothills of the Himalayas.

Method:

Four mixed-phase BMP schemes (Morrison, Lin, WDM6, and WSM6), which are parameterized with an increasing complexity from single to double moments of particle distribution to represent cloud processes, are used with an explicit convection permitting grid resolution (3 km x 3 km). Experiments are set up to simulate a convective storm that occurred in the late afternoon of 18th May 2011 and compared with i) Satellite-based tropical rainfall measuring mission (TRMM) 3B42 v7 data, and ii) Ground-based observations at Nagarkot (27.7°N, 85.5°E), Nepal.

Result:

Our results show that the simulated storm characteristics are not overly sensitive to the chosen BMP schemes. In general, all the BMP schemes produce similar rainfall characteristics and compares reasonably well with the observations across Siwalik Hills and Middle Mountains, which act as a topographic barrier to low level circulations and receive more rain. The schemes, however, show negative bias across central Nepal including the Kathmandu Valley, albeit the magnitude and spatial distribution of bias are different between the schemes. In contrast, upper level total water condensate and cloud fraction show a strong sensitivity to the BMP schemes.

Conclusion:

Overall, the Morrison scheme, in addition to warm clouds which also predict double moment distribution of all hydrometeors in the cold-cloud processes, a dominant cloud forming process in the Himalayas, accurately represents the mechanism and outperforms the simplified schemes based on root mean square error (RMSE) analysis.

Keywords: Himalayas, Cloud microphysics, Sensitivity analysis, Complex terrain, Nepal.

1. INTRODUCTION

One of the major uncertainties in numerical weather prediction (NWP) arises from inadequate representation of cloud microphysical processes in the NWP model [1 - 3]. Although high resolution model simulations are made

* Address correspondence to this author at the Canadian Center for Climate Modelling and Analysis (CCCma), Environment and Climate Change Canada, 3800 Finnerty Road, Victoria BC V8P 5C2, Canada; Tel: +1 7786761974; E-mail: rudrasha@gmail.com

possible by advanced computing facilities [4], accurate forecasting can't be guaranteed [5] which has been a primary concern while applying the NWP model in research and operational forecasting of weather. This task is even more challenging over the Himalayas due to the role of complex terrain, where general theory and findings from elsewhere may not be fully transferrable [6].

The giant Himalayas interact with moisture-rich air that generally originates in the Bay of Bengal and initiates topography-induced convection. This convective process is invigorated by a strong temperature gradient during pre-monsoon season (March – May) [7, 8] leading to the formation of cumulonimbus clouds, where the release of latent heat during the process further enhances the storm development [9 - 11]. The effects of such microphysical processes are significant in the cold phase of clouds which are considered as a dominant precipitation formation mechanism in mountainous region [12].

Sophisticated microphysical parameterization schemes have been developed in recent decades to represent cloud processes in the climate and weather model [13 - 15]. In the bin microphysics parameterization, evolution of particle size distribution (PSD) is explicitly resolved [16] consequently it demands a high computational cost. In the bulk scheme the PSD is represented by a function [14, 17], generally derived from in-situ measurements, which uses moments of particle distribution to estimate bulk quantities, such as mixing ratio (single moment) or both mixing ratio and number concentration (double moment). The bulk scheme is widely used in the cloud resolving simulations [18 - 21] due to high computational advantage [22].

In the bulk microphysical parameterizations (BMP) schemes, cloud processes are parameterized following a wide spectrum of hypothesis ranging from a very simple mechanism with few hydrometeor species [23] to a complex scheme involving very detailed representation of hydrometeors [22]. These wide varieties of cloud parameterizations regulate behavior of model physics which in turn causes the model sensitive to these schemes. Analysis of this sensitivity of model to different microphysical parameterization schemes help to improve our current understanding of cloud processes and also guide for future model development.

A number of studies have highlighted the sensitivity of cloud-resolving model to BMP schemes. According to Liu and Moncrieff [19], different storm characteristics were observed across the continental United States during simulations of a summer-time convective storm using four different BMP schemes, which represent range of cloud processes from simple ice (ice and liquid drop does not coexist) to mixed-phase. The degree of the model sensitivity was more pronounced to ice phase processes. Reisner *et al.* [24] evaluated the sensitivity of single and double moment microphysical parameterization schemes to cloud-resolving model (MM5) to predict super-cooled liquid water during the two winter storms across the Rocky Mountain and surrounding areas of Colorado. The simulated storms were sensitive to the chosen schemes and the double moment scheme was able to reproduce the observed storm characteristics in the both cases. A similar sensitivity was observed in the simulation of idealized stratiform precipitation [25] and also in the simulation of winter precipitation over the complex terrain of Colorado Headwater region [20].

In this paper, we aim to investigate microphysical dependence of simulated characteristics of a convective storm that generally develops during the pre-monsoon season over the foothills of the Himalayas. Such studies have been well documented over the continental United States [19, 20], North Atlantic Ocean [1] and Southeast India [21] however; it is poorly investigated over the Nepal Himalayas.

Section 2 of this paper describes experimental design and observation data. Simulations results and discussion are presented in section 3. Finally, summary and conclusions are drawn in section 4.

2. DATA AND EXPERIMENT DESIGN

A numerical experiment was carried out using the Weather Research and Forecasting (WRF) model version 3.1.1 with Advanced Research WRF (WRF-ARW) dynamical core [26]. The WRF is a non-hydrostatic, primitive equation model with vertical and horizontal wind components, microphysical quantities, perturbation potential temperature, geopotential and surface pressure of dry air as prognostic variables. The model was defined in the Lambert conformal projection and was configured with three two-way nested domains with a grid spacing of 27, 9 and 3 km centered over central Nepal (26.34° N, 83.12° E) as shown in (Fig. 1). The coarse domain covered most of the Hindu – Kush Himalaya region, the Indian subcontinent and the Bay of Bengal. The domain 2 is expanded to cover the whole Nepal including southern portion of the Tibetan plateau and northern part of India. The innermost domain, which covers mainly central Nepal including the Kathmandu Valley, contains 111×111 horizontal grid points and 40 vertical levels

with domain top pressure 50 mb. The model integration time-step was set to 30 s. We used NCEP/DOE reanalysis 2 data for the model initialisation and boundary conditions. The twenty-four categories of terrestrial data were obtained from the USGS ‘30s’ global data set (http://www.mmm.ucar.edu/wrf/users/download/get_source2.html). The model was initialized at 09 UTC on 17 May 2011 and ran for 39 hours. The first 6 hours simulation is generally considered as a spin-up run [21] hence last 33 hours was considered for the evaluation.

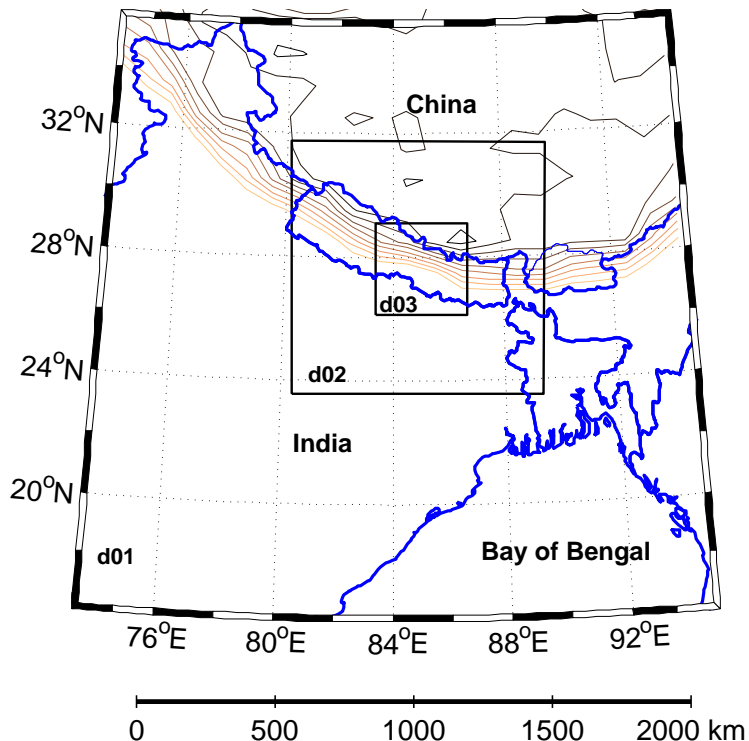


Fig. (1). Domains used for WRF simulations with horizontal grid resolution 27 km (domain 1), 9 km (domain 2) and 3 km (domain 3) centered over central Nepal (26.34° N, 83.12° E) and the model is set to 40 vertical levels.

The physics packages used in this study comprise the Dudhia short-wave radiation [27], the RRTM long-wave radiation [28], the YSU boundary layer [29] and the Noah land surface models [30]. The cumulus convection is explicitly resolved in the high resolution domain (3 km grid) but parameterized using the Grell-Devenyi scheme in the coarse domains.

Four microphysical schemes, which are parameterized with an increasing complexity to resolve water vapor, clouds and precipitation, were examined to analyze the sensitivity of a convective storm. The schemes considered are the Morrison double moment scheme [22, 25], the Lin scheme [14, 31], the WRF double moment 6-class scheme (WDM6) [15], and the WRF single moment 6-class scheme (WSM6) [23].

The Lin is a mixed-phase single moment bulk microphysics scheme which predicts mixing ratio of 6-class water substances: water vapour, cloud water, rain water, cloud ice, snow and graupel as a prognostic variable and assumes exponential size distribution of the five hydrometeor species. The WSM6, also a mixed-phase scheme, predicts mixing ratio of the 6-class water substance variables. The warm phase cloud processes in this scheme are very similar to the Lin scheme however ice parameterizations are somewhat different. The WDM6 scheme follows the WSM6 scheme and consist the same prognostic water substance variables. However, this is a double moment scheme for warm-phase clouds hence it predicts both mixing ratio and number concentration of the warm-phase hydrometeor species (i.e. cloud water and rain water). The Morrison is the most sophisticated double moment cloud microphysics scheme among the schemes considered in this study that predicts mixing ratio and number concentration of the five hydrometeor species and mixing ratio of water vapour. In contrast to the other schemes, the Morrison scheme includes the effects of aerosol whose concentration and characteristics can be prescribed in the model consequently determine cloud condensation nuclei (CCN) and droplets concentration.

We use ground-based and satellite-based observations of meteorological variables to evaluate performance of the

schemes. A meteorological monitoring station was set up at Nagarkot (Lon: 85.5°E, Lat: 27.7°N, Alt: 1900 m asl), Nepal. At this site a Vaisala meteorological sensor (Met Pack WTX 510) were installed on the roof top of a two storey building, which was approximately 5 m above the ground. The station was mounted on a mast offering good 360° exposure. The weather station recorded measurements of temperature, relative humidity, surface pressure, wind speed, wind direction and precipitation with rainfall and hail discriminations using piezoelectric sensor. The sensor was set to record the variables at 1 minute interval. Tropical rainfall measuring mission (TRMM) 3B42 version 7 (hereafter 3B42 v7) data was used to evaluate performance of the BMP schemes. The 3B42 v7 rainfall data is available at 3 hourly temporal and 0.25° x 0.25° spatial resolution which was interpolated to 3 km x 3 km grids over the study domain. Detail of the rainfall products can be found at Huffman *et al.* [32], Huffman and Bolvin [33] and the TRMM website (<http://pmm.nasa.gov/TRMM>). In order to address location error in a point-to-point comparison between observed and simulated data, average value of variables over adjoining grid boxes, which are located at west, east, south and north from a station, are considered.

Finally, we calculated the root mean square errors (RMSE), which allow us to compare simulated results with observation-based data, using the simulated ($X_{m,i}$) and observation-based ($X_{o,i}$) accumulated rainfall, temperature and wind speed. A spatial distribution of rainfall accumulated over 33 hours was used to estimate the RMSE with respect to the 3B42 v7 data, where in this case, n in the equation (1) is represented by total number of grid points across the study domain. However, temporal distribution of meteorological variables (e.g. 30 min accumulated rainfall, 30 min averaged temperature and wind speed) were used to calculate the RMSE with respect to the Nagarkot station where value of n is equal to 66, total number of model output during 33 hours of simulation.

$$RMSE = \sqrt{\frac{\sum_{i=1}^n (X_{o,i} - X_{m,i})^2}{n}} \quad (1)$$

3. RESULTS AND DISCUSSION

Results from the WRF simulations are shown in (Figs. 3 through 9). These figures explain the evolution of simulated meteorological variables and hydrometeor species. The simulated variables are compared with the ground-based observation and satellite-based 3B42 v7 data.

3.1. Details of the Convective Storm

The convective storm occurred in the late afternoon of 18 May, 2011. Infrared and visible spectra of the geostationary satellite (MET7) images show synoptic weather conditions associated with the convective storm (Fig. 2). The visible Fig. (2a) and infrared Fig. (2b) satellite images, which indicate amount of reflected solar radiation and cloud temperature respectively, were received at 0800 UTC 18 May 2011. Both satellite images show an evolution of thick clouds over central and eastern Nepal which is denoted by a red circle in the figures. Over the next three hours (i.e. 1100 UTC 18 May 2011) the clouds disappeared (Figs. 2c-d) after producing a heavy downpour which is consistent with observation at Nagarkot station Fig. (3f). The characteristics of surface meteorology is described in section 2.2 which includes dry bulb temperature, relative humidity, wind speed, wind direction, rainfall, and surface pressure.

3.2. Simulations of Surface Meteorology

Fig. (3) shows a comparison of the WRF simulated time series analysis of meteorological variables for the four microphysics schemes along with the observed meteorology at Nagarkot station. Surface temperature simulation showed a clear diurnal cycle with a magnitude of the peak temperature ~27 °C occurring around 2 pm local time (local time = UTC time + 5:45 hour) and lowest temperature simulated early in the morning Fig. (3a). All the schemes, generally overestimated the surface temperature at Nagarkot, simulated very similar profiles, which are consistent with the magnitude of the RMSE 3.2°, 3.0°, 3.0°, and 3.0° for the Morrison, Lin, WDM6 and WSM6, respectively. The observed peak temperature was recorded to be ~21 °C around 2 pm local time. Overestimated surface temperature can be attributed to underestimation of precipitation Fig. (3f) which is a result of less clouds cover, allowing more incoming solar radiation reaching to surface, and in turn, increase surface air temperature [34]. However, both the observed and simulated temperature profiles showed a drastic drop in environmental temperature as rainfall started which may be attributed to evaporative cooling mechanism [35]. In this process when raindrops fall below saturated layer, air cools from evaporation of raindrops and melting of hail particles. This cooling is also possible due to passage of cold fronts ahead of the storm [36]. For example, rapid cooling of environment with a magnitude of more than 7 °C per hour was found in southeast India due to passage of a cold front ahead of the thunderstorm [21].

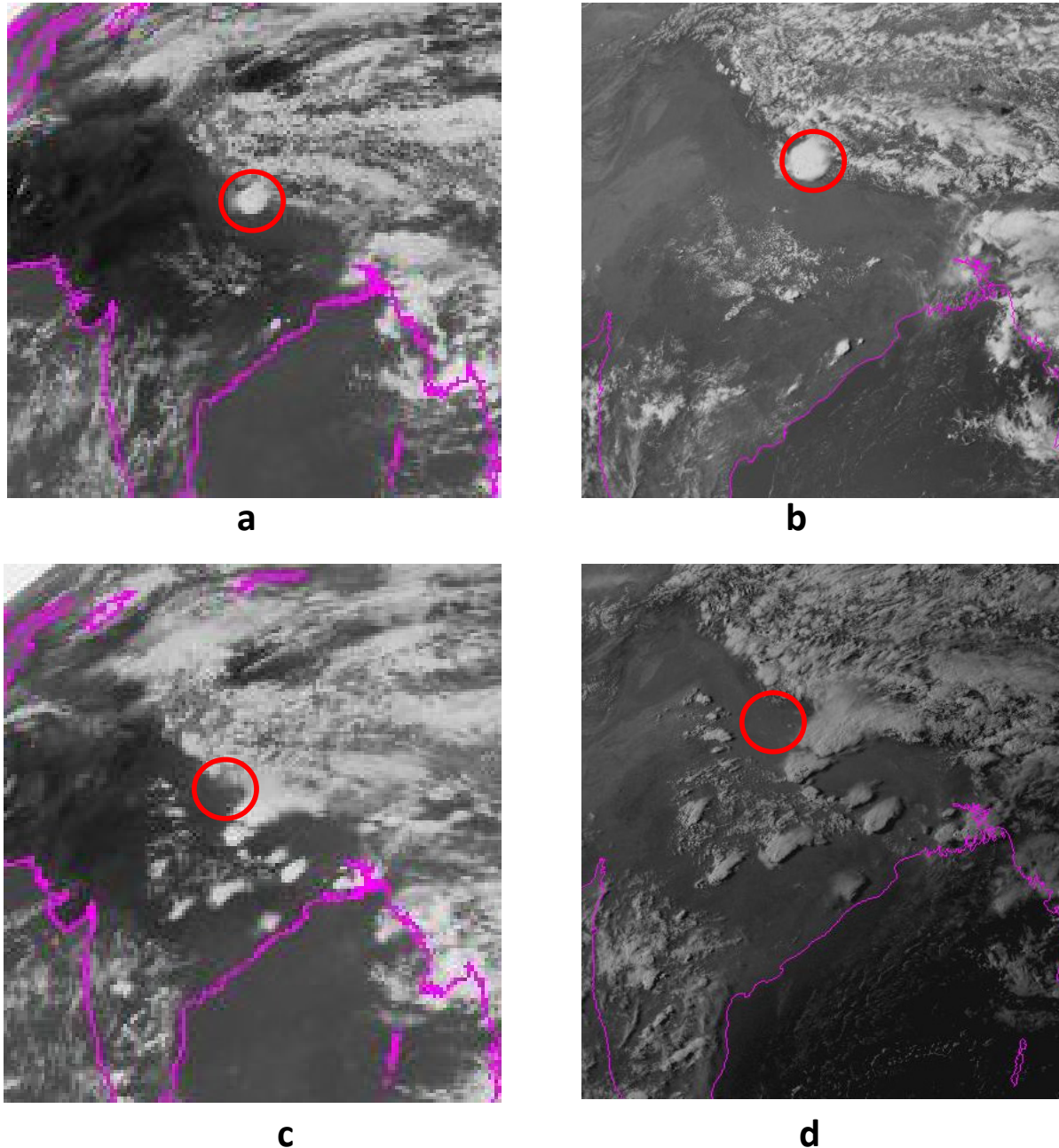


Fig. (2). Geostationary satellite (MET7) images (a) infrared, and (b) visible spectrum both received at 08 UTC 18 May 2011 (13:45 Local); (c) infrared, and (d) visible spectrum both received at 1100 UTC 18 May 2011 (16:45 Local).

Consistent with surface temperature, simulated relative humidity (RH) profile Fig. (3c) showed a minimum diurnal value (~40%) around 2 pm local time and reached maximum (~95%) early in the morning. The maximum and minimum observed RH were ~90% and ~71% respectively. The simulated RH was not sensitive to the chosen microphysics schemes, which produced identical profiles. Consistent with overestimation of temperature and underestimation of precipitation (explained below) the model underestimated the observed RH. Our analysis showed that the RH sharply increased before initiation of rainfall, which is consistent with formation of clouds and raindrops, in the both observed and simulated cases.

The simulated surface pressure profiles were identical Fig. (3e) which dropped from ~820 hPa to ~817 hPa before the precipitation and gradually increased after dissipation of the storm. This phenomenon is consistent with the observed surface pressure, although the model overestimated the mean surface pressure by 1%. Dai and Trenberth [37] report that the CCSM2 (Community Climate System Model) overestimated surface pressure by 20–50% over low-

latitude and underestimated by the same amount over mid-latitude which was associated with the model deficiencies in simulating tropical latent heat.

Fig. (3b) shows that the wind direction shifted from westerly to south-easterly wind before local midnight (1815 UTC) and came back to south-westerly in the afternoon. This pattern is similar for all the four microphysics schemes and suggested a non-sensitivity of wind direction to microphysical parameterization. The observed wind direction at this location is mostly easterly which is not usual in this season [38]. The model simulated a light wind (≤ 2 m/s) early in the morning and suddenly escalated to ~ 8 m/s in the afternoon Fig. (3d). The simulated wind speed profiles are very similar for all the four microphysics schemes which is consistent with the magnitude of RMSE 2.1, 2.1, 2.2, 2.0 m/s for the Morrison, Lin, WDM6 and WSM6, respectively, although the Lin scheme simulated slightly high wind velocity before the storm. The model generally underestimated the observed wind velocity where the maximum and minimum speeds were 6 m/s and 2 m/s, respectively and did not show any diurnal pattern.

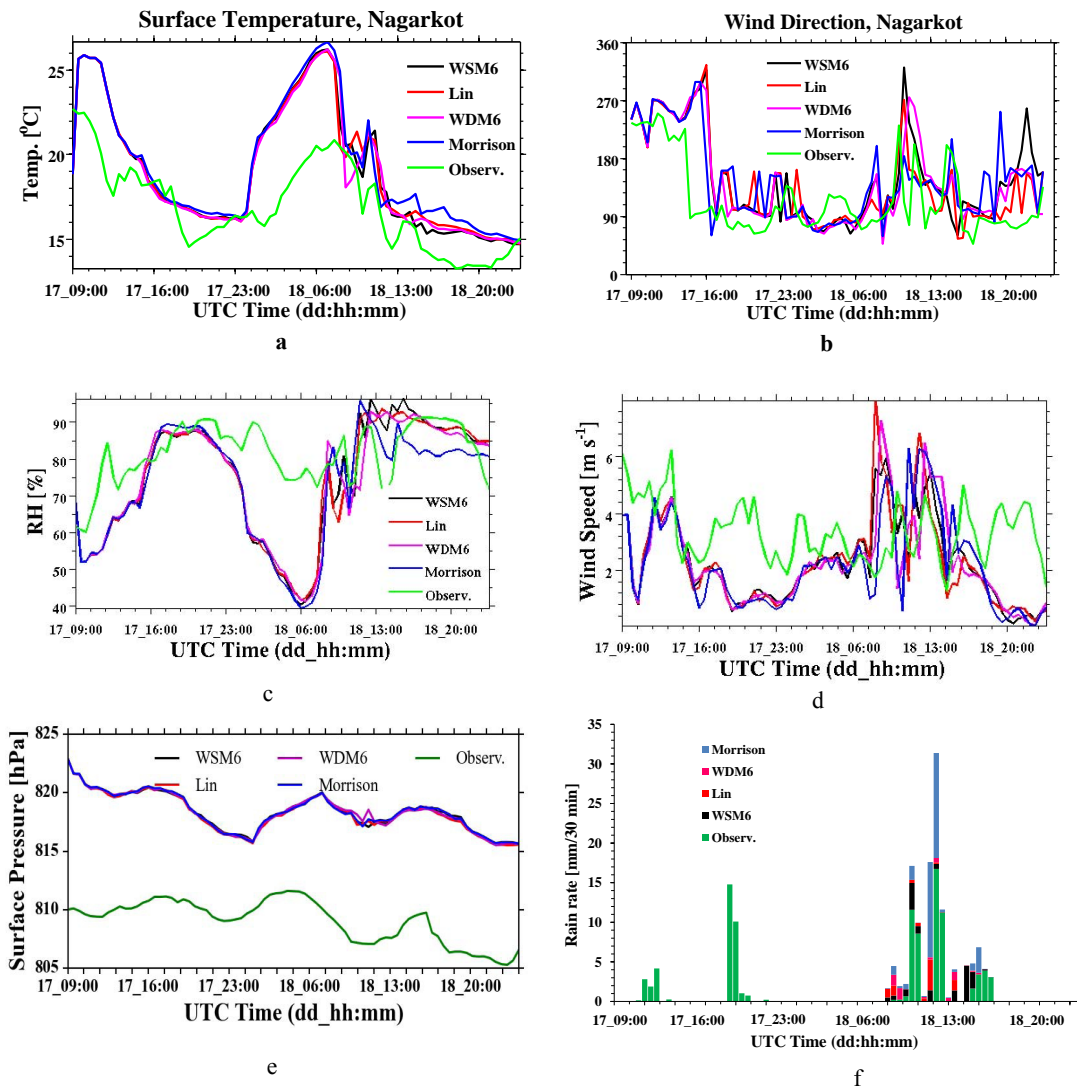


Fig. (3). Time series analysis of observed and simulated meteorological variables for the four microphysics schemes (a) surface temperature, and (b) relative humidity, (c) wind speed, (d) wind direction, (e) surface pressure, and (f) rainfall at Nagarkot, Nepal.

All the schemes underestimated the actual rainfall intensity and completely missed out some earlier episodes of rainfall event at Nagarkot Fig. (3f). Over 33 hours of simulation the model showed 34.20 mm, 9.10 mm, 16.60 mm, and 5.60 mm rainfall for the Morrison, Lin, WSM6, and WDM6 schemes, respectively. Rainfall amount over the same time period at the station was 88.33 mm and 57.07 mm based on ground-based measurement and 3B42 v7 data respectively also shown in Fig. (4b). Based on the RMSE (see parenthesis values in Table 1) the Morrison scheme performed better

than the other schemes. The disagreement between the ground-based observation and 3B42 v7 data can be explained in two ways. Firstly, the rain gauge observation themselves might have been affected by winds [39, 40] and other random sources of error and secondly, the systematic errors and coarse spatial resolution of the TRMM data set [39]. The latter causes strong underestimation of the TRMM rainfall in mountainous terrain [41 - 43], also observed in this study. The TRMM derived spatial distribution of 33 hours accumulated rainfall Fig. (4a) showed that eastern and central Nepal, mostly in Siwalik Hills and Middle Mountain range, receive more rainfall. The Middle Mountain region acts as a topographic barrier to low level circulations and greatly influence distribution of rainfall leading to more rain across southern part of the region [44, 45], and 3B42 v7 data also support this hypothesis.

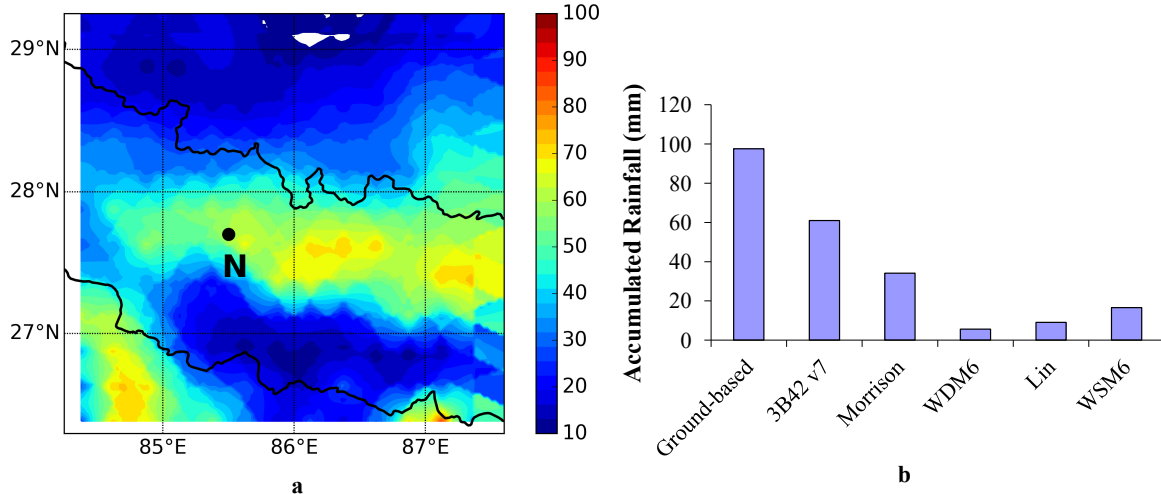


Fig. (4). 33 hours accumulated rainfall (mm) a) spatial distribution, represented by colour contours, over the study domain derived from the Tropical Rainfall Measuring Mission (TRMM) version 7 (3B42 v7) data. Ground-based measurement site (Nagarkot, Lat: 27.7 °N, Lon: 85.5 °E, Alt: 1900 m asl) is denoted by a black circle and a letter N, thick black line represents country boundary, and b) comparison between simulations and observations at Nagarkot station.

Table 1. Comparison of rainfall between simulations and observations (ground-based and satellite-based). RMSE values in parenthesis are relative to Nagarkot observation data.

Scheme	33 hours Accumulated Rainfall (mm)					RMSE (mm)
	Simulated (Nagarkot)	Ground-based observation (Nagarkot)	Satellite-based (Nagarkot)	Simulated (Domain Average)	Satellite-based (Domain Averaged)	
Morrison	34.20	88.33	57.07	6.03	29.14	28.0 (3.2)
Lin	9.10			6.58		29.0 (3.6)
WSM6	16.60			5.88		28.4 (3.4)
WDM6	5.60			5.17		29.1 (3.6)

Spatial distribution of rainfall biases, which are estimated taking difference between the simulated and 3B42 v7 rainfall over 33 hours, for the four microphysical parameterization schemes are shown in Fig. (5). All the schemes showed an identical distribution pattern with negative rainfall bias across central Nepal including the Kathmandu Valley which is consistent with the observations at Nagarkot Figs. (3f, 4b), although magnitude and spatial distribution of the bias are different among the schemes. On average, the Morrison scheme produced 6.03 mm rain across each model grid during 33 hours of simulation. Similarly, the Lin, WSM6 and WDM6 scheme generated 6.58 mm, 5.88 mm and 5.17 mm rain, respectively; however, the observation-based 3B42 v7 data showed 29.14 mm rain for the same time period (Table 1). Based on the RMSE (Table 1) the Morrison scheme, which shows the smallest error among the schemes, was closer to the observations. However, the WDM6 shows largest error among the schemes. The better performance of the Morrison scheme is attributed to prediction of double moment distribution of all hydrometeors in cold cloud processes which is a dominant cloud forming process in the Himalayas [12] and also showed in our simulations (explained below). In contrast, the poor performance of the WDM6 is due to prediction of double moment distribution of hydrometeors only in warm phase of clouds which in fact do not significantly contribute to form precipitation in the

Himalayas.

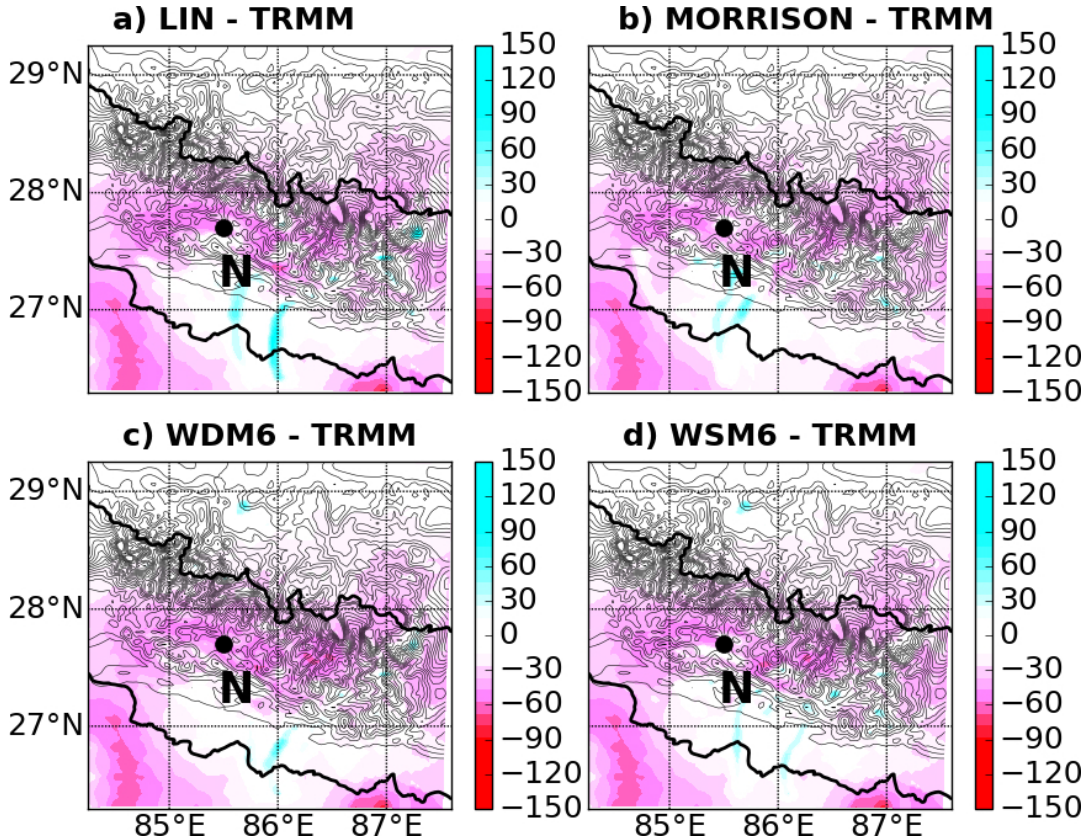


Fig. (5). Spatial distribution of rainfall biases with respect to TRMM 3B42 v7 data a) Lin - TRMM, b) Morrison - TRMM, c) WDM6 - TRMM, and d) WSM6 - TRMM. The Nagarkot measurement site is denoted by a black circle and a letter N. Line and colour contours represent topography and rainfall respectively and thick black line represents country boundary.

The forecast errors may be attributed to a coarse grid resolution ($3 \text{ km} \times 3 \text{ km}$) which may not be able to simulate detail features of the storm. In an explicit coarse grid resolution convective processes can be inhibited or delayed [19, 46] which could lead to a rapid growth of clouds and precipitation. However, those effects were not observed when convection permitting grid reduced to a finer resolution ($< 200 \text{ m}$) [46]. Secondly, the error may also be attributed to a lateral boundary condition as Liu and Moncrieff [19] argued that the MM5 model underestimated convective rainfall across the continental United States due to a smooth lateral boundary condition which was derived from 40 km Eta model analyses. In our study 3-hourly lateral boundary condition was interpolated from $2.5^\circ \times 2.5^\circ$ horizontal resolution and 17 pressure levels from the NCEP reanalysis data.

3.3. Simulations of Vertical Velocity

Fig. (6) shows evolution of vertical velocity with time and height simulated for the four microphysics scheme at Nagarkot. Strong updrafts and downdrafts, which play a role to determine intensity of precipitation and type of hydrometeors [47], are the typical characteristics of a convective storm. All the schemes simulated updrafts ($\sim 2 \text{ m/s}$) and associated downdrafts ($\sim 1.5 \text{ m/s}$) around 1600 UTC on 17th May and 0600 UTC on 18th May which is roughly consistent with the observed rainfall at this location, although the model completely missed out a convective event that occurred around 1730 UTC on 17th May. The convective cores could reach up to 15 km from the ground level. Although the schemes, in general, were able to capture timing of the convective initiation, surprisingly, none of the schemes reproduced the observed distribution of rainfall. As reported in Rajeevan *et al.* [21] this is related to strength of the simulated vertical velocity which was much weaker here to form a storm. The Morrison scheme simulated a stronger updraft core, which rose high up to 12 km from surface level, and was consistent with relatively more rainfall than its counterparts.

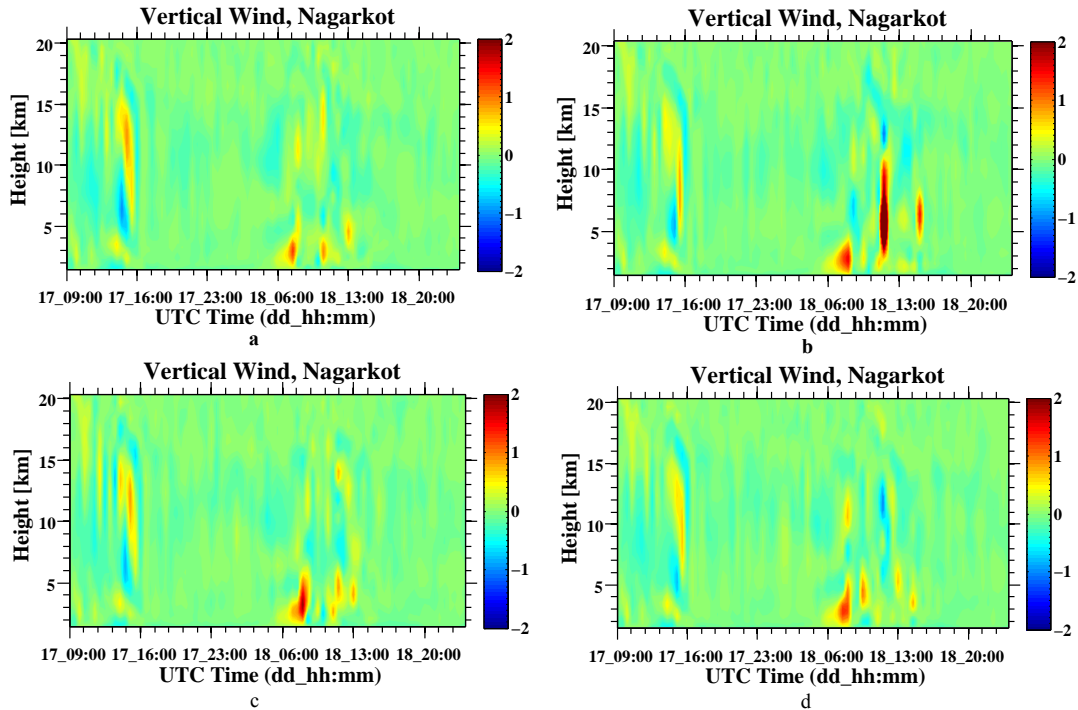


Fig. (6). Vertical velocity (m s^{-1}) at Nagarkot station, simulated for the four microphysical parameterization schemes (a) Lin, (b) Morrison, (c) WDM6, and (d) WSM6 scheme.

Fig. (7) shows zonal averaged wind simulated for the four microphysics schemes at $\sim 5 \text{ km}$ from ground level. All the schemes showed a northward propagation of convection with strong updrafts and downdrafts in the beginning and near the end of simulations. The updrafts track showed a strong dependency of convection on the topography because strong updrafts were observed when the storm moved towards the high elevation terrain (i.e. northward).

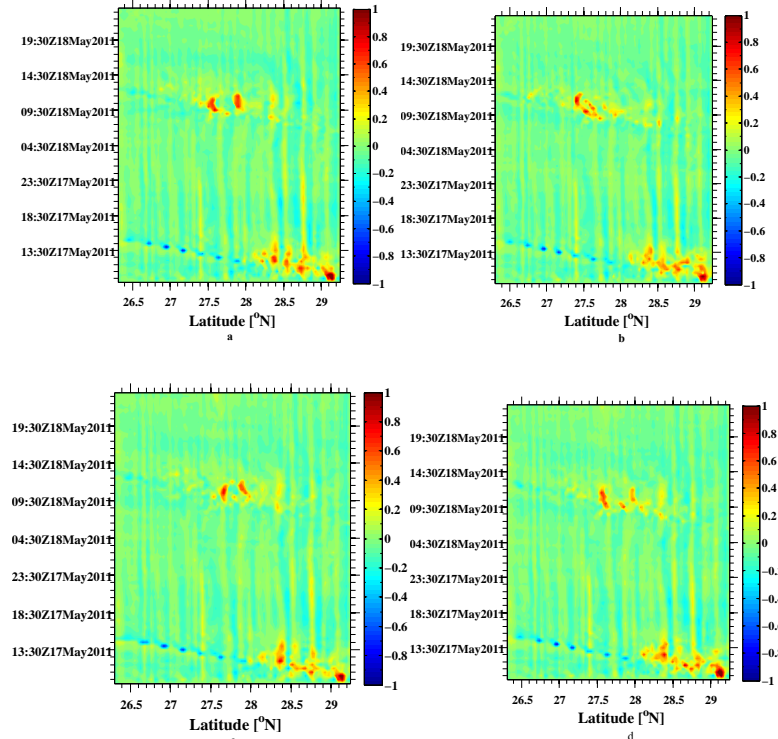


Fig. (7). Time – latitude diagrams for vertical velocity at a mean height of $\sim 5 \text{ km}$ from the ground level simulated for (a) Lin, (b) Morrison, (c) WDM6, and (d) WSM6 scheme.

3.4. Simulations of Hydrometeor Profile

Figs. (8a and b) show domain and time averaged vertical profiles of total water condensate (hereafter condensate) and cloud fraction respectively simulated for the four microphysical schemes. The condensate in a grid box was calculated by adding up mixing ratio of hydrometeors (cloud water, cloud ice, rain water, snow and graupel) present in the grid. The cloud fraction, computed based on mixing ratio of hydrometers, is adopted from Liu and Moncrieff [19], which assumes 100% cloudiness over a grid box when sum of cloud water, ice and snow mixing ratio exceeds 0.01 g/kg.

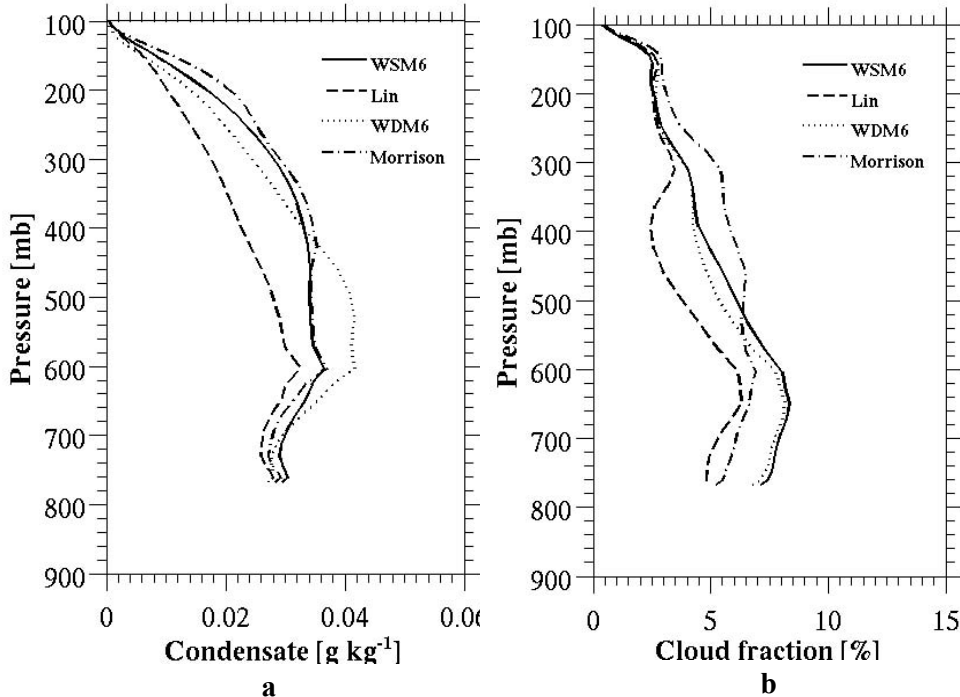


Fig. (8). Domain and time averaged (a) total water condensate (g kg^{-1}), and (b) cloud fraction (%) simulated for the four microphysical parameterization schemes.

An identical vertical profile, gradual increment with height, of condensate was simulated for all the four schemes in the lower troposphere (below 600 hPa) Fig. (8a). However, significantly different profiles of the condensate among the four schemes were found in the upper troposphere. The Lin scheme produced minimum amount of the condensate and consequently the cloud fraction all the way from surface level to the upper atmosphere. The WDM6 scheme produced maximum condensate ($\sim 0.04 \text{ g/kg}$) in the middle of the atmosphere (400 hPa – 600 hPa). The Morrison scheme, which simulated maximum condensate ($\sim 0.036 \text{ g/kg}$) and cloud fraction ($\sim 7\%$) at $\sim 600 \text{ hPa}$ pressure level, showed higher condensate and cloud fraction profile than their counterparts in the upper atmosphere (above 500 hPa).

The disagreements among the schemes are attributed to different assumptions in the parameterization processes. For example, the schemes use different graupel densities which affect fall speed of particles [48] and consequently have the impacts on collision and coalescence processes [49]. The schemes also use different intercept parameters, which control slope of a function, to estimate distribution of hydrometeors in the both warm and cold phase processes. The variability in cloud cover may have been due to different approaches used in the parameterization of ice sedimentation processes and collection efficiency. For example, a high collection efficiency of ice causes fast transformation of cloud ice to snow which subsequently precipitate out due to its large sedimentation velocity [50]. Such effect was observed in the study of a deep tropical convection, where the WRF simulated anvil clouds was found less persistent than the observed clouds [51].

Fig. (9) shows the domain and time averaged vertical profiles of individual hydrometeor simulated for the four microphysics schemes. The profiles showed noticeable variations in hydrometeors' profile and more pronounced differences were observed in the cold phase of cloud processes, which is considered as a dominant cloud forming processes in the Himalayas. The strong sensitivity of the schemes with ice phase hydrometeors is attributed to moment

of distribution of hydrometeor particles represented in the schemes. For example, the Morrison scheme, which represents the detailed ice phase processes and consistent with the better performance as shown in RMSE, predicts number concentrations and mixing ratios of every ice phase hydrometeor particles. In contrast, the WDM6 scheme, which shows the poor performance among the schemes, predicts number concentrations and mixing ratios of hydrometeors only for warm cloud processes, which is less likely to occur in the Himalayas. The model simulated identical profiles of rainwater mixing ratio (q_r) for all the schemes with $\sim 0.008 \text{ g/kg}$ at the surface level and remained constant with height up to 500 hPa, although the WDM6 scheme produced slightly more rainwater in the middle atmosphere ($\sim 500 \text{ hPa} - 600 \text{ hPa}$). Distribution of cloud water mixing ratio (q_c) exhibited a similar evolution pattern; however, magnitudes are somewhat different among the schemes, where the Morrison (WDM6) scheme simulated a highest (lowest) mixing ratio profile. All the schemes simulated negligible ice mixing ratio (q_i) that may be attributed to a rapid transformation of ice to snow and graupel as explained above. In the Morrison scheme, snow mixing ratio (q_s), which was the highest among the schemes, was dominated over graupel mixing ratio (q_g), which was the lowest among the schemes. In contrast, the opposite was true for the other three schemes. A number of other studies have also highlighted significant variations in mixing ratio of hydrometeors among different microphysical parameterization schemes [19 - 21].

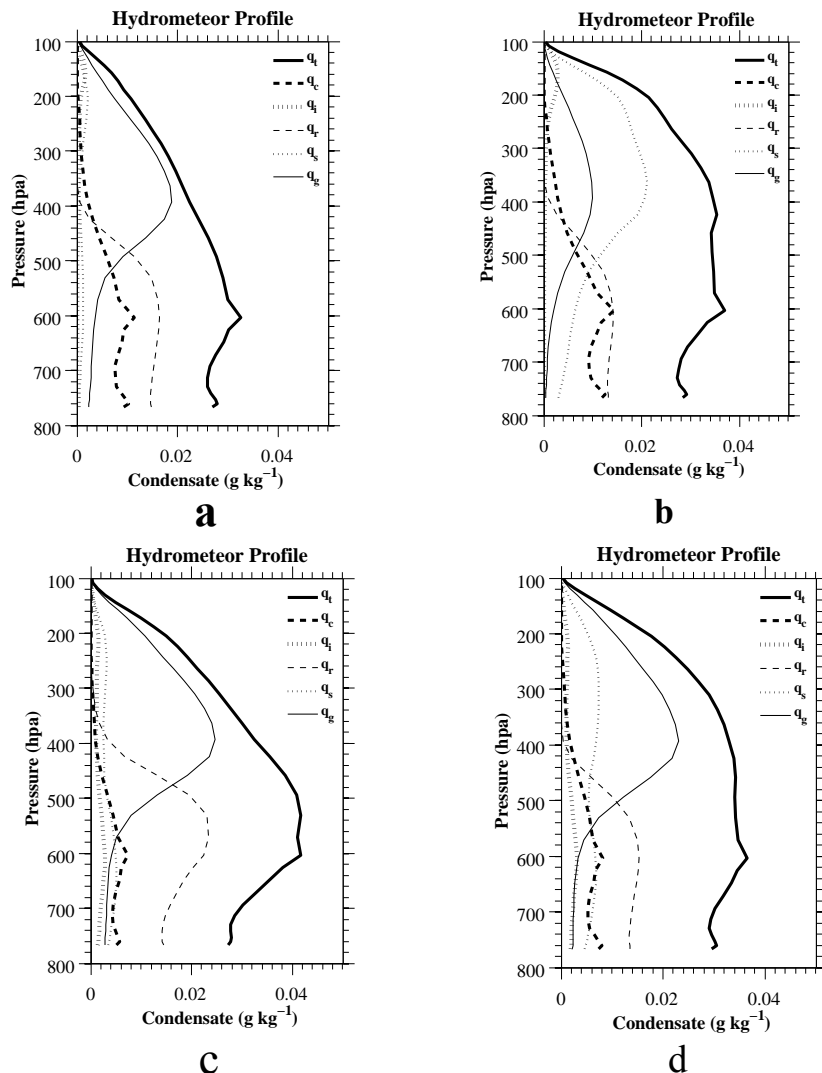


Fig. (9). Domain and time averaged vertical profiles of cloud water (q_c , thick dashed), rainwater (q_r , dashed), ice (q_i , thick dotted), snow (q_s , dotted), graupel (q_g , solid) and total condensate (q_t , thick solid) mixing ratio (g kg^{-1}) simulated for (a) Lin, (b) Morrison, (c) WDM6, and (d) WSM6 scheme.

4. SUMMARY AND CONCLUSIONS

We carried out a sensitivity analysis of four bulk microphysical parameterization (BMP) schemes (Morrison, Lin, WDM6, and WSM6) to simulate a convective storm, which generally develops during per-monsoon (March – May) season over the foothills of the Himalayas, using a high resolution (3 km x 3 km) configuration of WRF model. The study domain is characterized by a complex terrain of the Himalayas including the Mt. Everest (8,848 m) in the north and ‘Terai’ (low land in southern Nepal, altitude < 200 m) in the south. A convective storm that evolved mainly over central Nepal in the late afternoon of 18 May, 2011 was considered in this study. To evaluate performance of the model, simulation results are compared with a high temporal resolution (1 min.) dataset obtained from an observation station which was set up at Nagarkot (Lat: 27.7°N, Lon: 85.5°E, Alt: 1900 m asl), Nepal as part of this study. Furthermore, the latest version (v7) of tropical rainfall measuring mission (TRMM) satellite data (3B42 v7), which is available at 3 hourly temporal and $0.25^\circ \times 0.25^\circ$ spatial resolution, was interpolated onto the model grids to compare with the simulations. Bias and root mean square error (RMSE) are calculated to evaluate the performance of the four BMP schemes.

The BMP schemes considered here are parameterized with an increasing complexity, from a single to double moments of particle distribution. The schemes make different assumptions to represent cloud microphysical processes in the model. Evaluation of the BMP schemes are based on analysis of temporal and spatial distribution of meteorological variables, vertical profiles of hydrometeors, updrafts and downdrafts and cloud cover. Major results are summarized as below:

- All the BMP schemes show negative bias across central Nepal, based on 3B42 v7 data, although the magnitude and spatial distribution of biases are different between the schemes. The RMSE for rainfall suggest that the Morrison scheme, which showed the smallest magnitude of error, was closer to the ground-based (Nagarkot) and satellite-based (3B42 v7) observations. The Morrison scheme, in addition to the warm phase clouds, also predicts number concentration and mixing ratio of all cold hydrometeors [22] that increase degree of freedom and improve radiative transfer calculations [52] in turn improve cold cloud processes, which is a dominant precipitation formation mechanism in the Himalayas [12] and accurately represents the mechanism. The RMSEs for surface temperature and wind speed, however, were very similar between the schemes.
- The Siwalik Hills and Middle Mountain range, where the simulated and 3B42 v7 rainfall rate agrees reasonably well, act as a topographic barrier for low level circulation and significantly influence formation and distribution of rainfall, receives more rain [44, 45]. Our simulations also support this hypothesis that all the BMP schemes produce more rain across the Siwalik Hills and Middle Mountain area.
- We observe that there are significant differences between the ground-based and satellite-based rainfalls at Nagarkot which may be attributed to i) the effects of wind on the ground-based instrument, and ii) systematic errors in the retrieval algorithm and coarse spatial coverage ($0.25^\circ \times 0.25^\circ$) of the TRMM satellite. The effects of the latter are more pronounced in mountainous terrain, which significantly underestimates the actual rainfall intensity [41 - 43]. Hence this research, which showed inconsistency between the ground-based and the TRMM derived rainfall intensity, supports the previous studies.
- A strong sensitivity of ice phase hydrometeors and cloud cover to the chosen BMP schemes is observed. Ice mixing ratio (q_i) in the WDM6 scheme was the highest among the schemes. The Morrison scheme simulated highest snow mixing ratio (q_s), whereas graupel content was the lowest. Further, the Morrison scheme generated maximum cloudiness in the upper troposphere and minimum cloudiness in the lower troposphere.

Our conclusions are based on the analysis of a single convective event which is the caveat of this study. However, this study indicates that improved ice processes in the model can significantly improve our understanding of precipitation processes over the Himalayas. It would also be more effective to carry out simulations of several other convective events covering diverse synoptic conditions and considering different physical processes such as boundary layer and land surface schemes. It would be interesting to look at the simulations with parameterized cumulus convection in the high resolution domain. A strong sensitivity of model to a parameterized cumulus convection than an explicit convection was found across the continental United States [53]. A convection permitting simulation configured with single domain could produce better results than multiple domains with parameterized convection in coarse and explicit convection in high resolution domain because parameterized convection in outer domain could influence inner domains [19, 21]. The single domain approach, however, could enhance errors while feeding coarse resolution data from a global model directly to high resolution grid [54].

CONFLICT OF INTEREST

The authors declare no conflict of interest, financial or otherwise.

ACKNOWLEDGEMENTS

This project was carried out under the funding of the Sustainable Consumption Institute (SCI), University of Manchester. The authors would like to thank SCI for PhD funding.

REFERENCES

- [1] Otkin JA, Greenwald TJ. Comparison of WRF Model-Simulated and MODIS-Derived Cloud Data. *Mon Weather Rev* 2008; 136: 1957-70.
[<http://dx.doi.org/10.1175/2007MWR2293.1>]
- [2] Weverberg KV, Lipzg NP, Delobbe L, Lauwaet D. Sensitivity of quantitative precipitation forecast to soil moisture initialization and microphysics parametrization. *Q J R Meteorol Soc* 2010; 136: 978-96.
[<http://dx.doi.org/10.1002/qj.611>]
- [3] Gultepe I. Mountain weather: observation and modeling. *Adv Geophys* 2015; 56: 229-312.
[<http://dx.doi.org/10.1016/bs.agph.2015.01.001>]
- [4] Nichols J, Kang S, Post W, Wang D, Bandaru V, Manowitz D, *et al.* HPC-EPIC for high resolution simulations for environmental and sustainability assessment. *Comput Electron Agric* 2011; 79: 112-5.
[<http://dx.doi.org/10.1016/j.compag.2011.08.012>]
- [5] Zheng Y, Alapaty K, Herwehe JA, Del Genio AD, Niyogi D. Improving high-resolution weather forecasts using the Weather Research and Forecasting (WRF) model with an updated Kain-Fritsch scheme. *Mon Weather Rev* 2016; 144: 833-60.
[<http://dx.doi.org/10.1175/MWR-D-15-0005.1>]
- [6] Panday AK. The Diurnal Cycle of Air Pollution in the Kathmandu Valley. Nepal: Massachusetts Institute of Technology 2006.
- [7] Gautam R, Hsu NC, Lau K-M, Tsay S-C, Kafatos M. Enhanced pre-monsoon warming over the Himalayan-Gangetic region from 1979 to 2007. *Geophys Res Lett* 2009; 36: L07704.
[<http://dx.doi.org/10.1029/2009GL037641>]
- [8] Lau K-M, Kim MK, Kim KM. Asian summer monsoon anomalies induced by aerosol direct forcing: the role of the Tibetan Plateau. *Clim Dyn* 2006; 26: 855-64.
[<http://dx.doi.org/10.1007/s00382-006-0114-z>]
- [9] Andreae MO, Rosenfeld D, Artaxo P, *et al.* Smoking rain clouds over the Amazon. *Science* 2004; 303(5662): 1337-42.
[<http://dx.doi.org/10.1126/science.1092779>] [PMID: 14988556]
- [10] Garabowski WW, Wu X, Moncrieff MW. Cloud Resolving Modeling of Tropical Cloud Systems during Phase III of GATE. Part III: Effects of Cloud Microphysics. *J Atmos Sci* 1999; 56: 2384-402.
[[http://dx.doi.org/10.1175/1520-0469\(1999\)056<2384:CRMOTC>2.0.CO;2](http://dx.doi.org/10.1175/1520-0469(1999)056<2384:CRMOTC>2.0.CO;2)]
- [11] Khain A, Rosenfeld D, Pokrovsky A. Aerosol impact on the dynamics and microphysics of deep convective clouds. *Q J R Meteorol Soc* 2005; 131: 2639-63.
[<http://dx.doi.org/10.1256/qj.04.62>]
- [12] Chen J-P, Lamb D. Simulation of Cloud Microphysical and Chemical Processes Using a Multicomponent Framework. Part II: Microphysical Evolution of a Wintertime Orographic Cloud. *J Atmos Sci* 1999; 56: 2293-312.
[[http://dx.doi.org/10.1175/1520-0469\(1999\)056<2293:SOCMAC>2.0.CO;2](http://dx.doi.org/10.1175/1520-0469(1999)056<2293:SOCMAC>2.0.CO;2)]
- [13] Morrison H, Curry JA, Shupe MD, Zuidema P. A new double-moment microphysics parameterization for application in clouds and climate models. Part II: single-column modeling for Arctic clouds. *J Atmos Sci* 2005; 62: 1678-93.
[<http://dx.doi.org/10.1175/JAS3447.1>]
- [14] Lin Y-L, Farrell RD, Orville HD. Bulk Parameterization of the Snow Field in a Cloud Model. *J Clim Appl Meteorol* 1983; 22: 1065-92.
[[http://dx.doi.org/10.1175/1520-0450\(1983\)022<1065:BPOTSF>2.0.CO;2](http://dx.doi.org/10.1175/1520-0450(1983)022<1065:BPOTSF>2.0.CO;2)]
- [15] Lim K-S, Hong S-Y. Development of an effective double-moment cloud microphysics scheme with prognostic Cloud Condensation Nuclei (CCN) for weather and climate models. *Mon Weather Rev* 2010; 138: 1587-612.
[<http://dx.doi.org/10.1175/2009MWR2968.1>]
- [16] Feingold G, Stevens B, Cotton WR, Walko RL. An explicit cloud microphysics/LES model designed to simulate the Twomey effect. *Atmos Res* 1994; 33: 207-33.
[[http://dx.doi.org/10.1016/0169-8095\(94\)90021-3](http://dx.doi.org/10.1016/0169-8095(94)90021-3)]
- [17] Rutledge SA, Hobbs PV. The mesoscale and microscale structure and organization of clouds and precipitation in midlatitude cyclones. VIII: A model for the “seeder–feeder” process in warm-frontal rainbands. *J Atmos Sci* 1983; 40: 1185-206.
[[http://dx.doi.org/10.1175/1520-0469\(1983\)040<1185:TMAMSA>2.0.CO;2](http://dx.doi.org/10.1175/1520-0469(1983)040<1185:TMAMSA>2.0.CO;2)]
- [18] Hong S-Y, Lim K-S, Kim J-H, Lim J-O, Dudhia J. Sensitivity Study of Cloud-Resolving Convective Simulations with WRF Using Two Bulk Microphysical Parameterizations: Ice-Phase Microphysics versus Sedimentation Effects. *J Appl Meteorol Climatol* 2009; 48: 61-76.
[<http://dx.doi.org/10.1175/2008JAMC1960.1>]

- [19] Liu C, Moncrieff MW. Sensitivity of Cloud-Resolving Simulations of Warm-Season Convection to Cloud Microphysics Parameterizations. *Mon Weather Rev* 2007; 135: 2854-68.
[<http://dx.doi.org/10.1175/MWR3437.1>]
- [20] Liu C, Ikeda K, Thompson G, Rasmussen R, Dudhia J. High-Resolution Simulations of Wintertime Precipitation in the Colorado Headwaters Region: Sensitivity to Physics Parameterizations. *Mon Weather Rev* 2011; 139: 3533-53.
[<http://dx.doi.org/10.1175/MWR-D-11-00009.1>]
- [21] Rajeevan M, Kesarkar A, Rao TN, Radhakrishna B, Rajasekhar M. Sensitivity of WRF cloud microphysics to simulations of a severe thunderstorm event over Southeast India. *Ann Geophys* 2010; 28: 603-19.
[<http://dx.doi.org/10.5194/angeo-28-603-2010>]
- [22] Morrison H, Curry JA, Khvorostyanov VI. A New Double-Moment Microphysics Parameterization for Application in Cloud and Climate Models. Part I: Description. *J Atmos Sci* 2005; 62: 1665-77.
[<http://dx.doi.org/10.1175/JAS3446.1>]
- [23] Hong S-Y, Dudhia J, Chen S-H. A Revised Approach to Ice Microphysical Processes for the Bulk Parameterization of Clouds and Precipitation. *Mon Weather Rev* 2004; 132: 103-20.
[[http://dx.doi.org/10.1175/1520-0493\(2004\)132<0103:ARATIM>2.0.CO;2](http://dx.doi.org/10.1175/1520-0493(2004)132<0103:ARATIM>2.0.CO;2)]
- [24] Reisner J, Rasmussen RM, Bruintjes RT. Explicit forecasting of supercooled liquid water in winter storms using the MM5 mesoscale model. *Q J R Meteorol Soc* 1998; 124: 1071-107.
[<http://dx.doi.org/10.1002/qj.49712454804>]
- [25] Morrison H, Thompson G. Impact of Cloud Microphysics on the Development of Trailing Stratiform Precipitation in a Simulated Squall Line: Comparison of One- and Two-Moment Schemes. *Mon Weather Rev* 2009; 137: 991-1007.
[<http://dx.doi.org/10.1175/2008MWR2556.1>]
- [26] Skamarock WC, Klemp JB, Dudhia J, Grill DO, Barker DM, Duda MG, et al. A Description of the Advanced Research WRF Version 3, NCAR Tech Note NCAR/TN 475 STR, UCAR Communications, Boulder, Colo 2008.
- [27] Dudhia J. Numerical study of convection observed during the winter monsoon experiment using a mesoscale two-dimensional model. *J Atmos Sci* 1989; 46: 3077-107.
[[http://dx.doi.org/10.1175/1520-0469\(1989\)046<3077:NSOCOD>2.0.CO;2](http://dx.doi.org/10.1175/1520-0469(1989)046<3077:NSOCOD>2.0.CO;2)]
- [28] Mlawer E, Taubman SJ, Brown PD, Iacono MJ, Clough SA. Radiative transfer for inhomogeneous atmosphere: RRTM, a validated correlated-k model for the longwave. *J Geophys Res* 1997; 102: 16663-82.
[<http://dx.doi.org/10.1029/97JD00237>]
- [29] Hong SY, Noh Y, Dudhia J. A new vertical diffusion package with an explicit treatment of entrainment processes. *Mon Weather Rev* 2006; 143: 2318-41.
[<http://dx.doi.org/10.1175/MWR3199.1>]
- [30] Ek MB, Mitchell KE, Lin Y, Rodgers E, Grunman P, Koren V, et al. Implementation of Noah land surface model advances in the National Center for Environmental Prediction operational mesoscale Eta model. *J Geophys Res* 2003; 108(D22): 8851.
[<http://dx.doi.org/10.1029/2002JD003296>]
- [31] Rutledge SA, Hobbs PV. The mesoscale and microscale structure and organization of clouds and precipitation in midlatitude cyclones. XII: A diagnostic modeling study of precipitation development in narrow cloud-frontal rainbands. *J Atmos Sci* 1984; 20: 2949-72.
[[http://dx.doi.org/10.1175/1520-0469\(1984\)041<2949:TMAMSA>2.0.CO;2](http://dx.doi.org/10.1175/1520-0469(1984)041<2949:TMAMSA>2.0.CO;2)]
- [32] Huffman GJ, Adler RF, Bolvin DT, Gu G, Nelkin EJ, Bowman KP, et al. The TRMM multi-satellite precipitation analysis: Quasi-global, multi-year, combined-sensor precipitation estimates at fine scale. *J Hydrometeorol* 2007; 8: 38-55.
[<http://dx.doi.org/10.1175/JHM560.1>]
- [33] Huffman GJ, Bolvin DT. TRMM and other data precipitation data set documentation. NASA, Greenbelt, USA. 2013.
- [34] Jin J, Miller NL, Schlegel N. Sensitivity study of four land surface scheme in the WRF model 2010.
[<http://dx.doi.org/10.1155/2010/167436>]
- [35] Ahrens CD. *Essentials of Meteorology: An invitation to the Atmosphere* 6 ed Belmont, USA: Brooks/Cole, Cengage Learning. 2012.
- [36] Wallace J, Hobbs P. *Atmospheric Science: An introduction survey* 2 ed London: Elsevier Inc. 2006.
- [37] Dai A, Trenberth KE. The diurnal cycle and its depiction in the community climate system model. *J Clim* 2004; 17: 930-51.
[[http://dx.doi.org/10.1175/1520-0442\(2004\)017<0930:TDCAID>2.0.CO;2](http://dx.doi.org/10.1175/1520-0442(2004)017<0930:TDCAID>2.0.CO;2)]
- [38] Shrestha RK, Gallagher MW, Connolly PJ. Diurnal and seasonal variations of meteorology and aerosol concentration in the foothills of the Nepal Himalayas (Nagarkot: 1,900 m asl). *Asia-Pac J Atmospheric Sci* 2016; 52: 63-75.
[<http://dx.doi.org/10.1007/s13143-016-0002-3>]
- [39] Chen Y, Ebert EE, Walsh KJ, Davidson NE. Evaluation of TRMM 3B42 precipitation estimates of tropical cyclone rainfall using PACRAIN data. *J Geophys Res* 2013; 118: 2184-96.
- [40] Duchon CE. Comparative rainfall observations from pit and aboveground rain gauges with and without wind shields. *Water Resour Res* 2001; 37: 3253-63.
[<http://dx.doi.org/10.1029/2001WR000541>]

- [41] Scheel ML, Rohrer M, Huggel C, Villar DS, Silvestre E, Huffman GJ. Evaluation of TRMM Multi-satellite precipitation analysis (TMPA) performance in the central Andes region and its dependency on spatial and temporal resolution. *Hydrol Earth Syst Sci* 2011; 15: 2649-63.
[<http://dx.doi.org/10.5194/hess-15-2649-2011>]
- [42] Prat OP, Barros AP. Assessing satellite-based precipitation estimate in Southern Appalachian mountains using rain gauges and TRMM PR. *Adv Geosci* 2010; 25: 143-53.
[<http://dx.doi.org/10.5194/adgeo-25-143-2010>]
- [43] Javannard S, Yatagai A, Nodzu MI, BodaghJamali J, Kawamoto H. Comparing high-resolution gridded precipitation data with satellite rainfall estimates of TRMM_3B42 over Iran. *Adv Geosci* 2010; 25: 119-25.
[<http://dx.doi.org/10.5194/adgeo-25-119-2010>]
- [44] Nayava JL. Rainfall in Nepal. *The Himalayan Review*: Nepal Geographical Society. 1980;12:1-18.
- [45] Kansakar SR, Hannah DM, Gerrard J, Rees G. Spatial pattern in the precipitation regime of Nepal. *Int J Climatol* 2004; 24: 1645-59.
[<http://dx.doi.org/10.1002/joc.1098>]
- [46] Petch JC. Sensitivity studies of developing convection in a cloud-resolving model. *Q J R Meteorol Soc* 2006; 132: 345-58.
[<http://dx.doi.org/10.1256/qj.05.71>]
- [47] Nelson S. The influence of storm flow structure on hail growth. *J Atmos Sci* 1983; 40: 1965-83.
[[http://dx.doi.org/10.1175/1520-0469\(1983\)040<1965:TIOSFS>2.0.CO;2](http://dx.doi.org/10.1175/1520-0469(1983)040<1965:TIOSFS>2.0.CO;2)]
- [48] Zikmund J, Vali G. Fall patterns and fall velocity of rimed ice crystals. *J Atmos Sci* 1972; 29: 1334-47.
[[http://dx.doi.org/10.1175/1520-0469\(1972\)029<1334:FPAFVO>2.0.CO;2](http://dx.doi.org/10.1175/1520-0469(1972)029<1334:FPAFVO>2.0.CO;2)]
- [49] Stensrud DJ. Parameterization schemes: Keys to understanding numerical weather prediction models. New York: Cambridge University Press 2009.
- [50] Pruppacher HR, Klett JD. *Microphysics of Clouds and Precipitation* 2 ed Dordrecht, The Netherlands: Kluwer Academic Publishers. 1997.
- [51] Connolly PJ, Vaughan G, May PT, Chemel C, Allen G, Choularton TW, *et al.* Can aerosols influence deep tropical convection? Aerosol indirect effects in the Hector island thunderstorm. *Q J R Meteorol Soc* 2011; 139: 2190-208.
[<http://dx.doi.org/10.1002/qj.2083>]
- [52] Meyers MP, Walko RL, Harrington JY, Cotton WR. New RAMS cloud microphysics parameterization. Part II: The two-moment scheme. *Atmos Res* 1997; 45: 3-39.
[[http://dx.doi.org/10.1016/S0169-8095\(97\)00018-5](http://dx.doi.org/10.1016/S0169-8095(97)00018-5)]
- [53] Liu C, Moncrieff MW, Tuttle JD, Carbone RE. Explicit and parameterized episodes of warm-season precipitation over the continental United States. *Adv Atmos Sci* 2006; 23: 91-105.
[<http://dx.doi.org/10.1007/s00376-006-0010-9>]
- [54] Leung LR, Qian Y. The Sensitivity of Precipitation and Snowpack Simulations to Model Resolution via Nesting in Regions of Complex Terrain. *J Hydrometeorol* 2003; 4: 1025-43.
[[http://dx.doi.org/10.1175/1525-7541\(2003\)004<1025:TSOPAS>2.0.CO;2](http://dx.doi.org/10.1175/1525-7541(2003)004<1025:TSOPAS>2.0.CO;2)]

© 2017 Shrestha *et al.*

This is an open access article distributed under the terms of the Creative Commons Attribution 4.0 International Public License (CC-BY 4.0), a copy of which is available at: <https://creativecommons.org/licenses/by/4.0/legalcode>. This license permits unrestricted use, distribution, and reproduction in any medium, provided the original author and source are credited.